The reactive extrusion of thermoplastic polyurethane

Verhoeven, Vincent Wilhelmus Andreas

4 A comparison of different measurement methods for the kinetics of polyurethane polymerization

4.1 Introduction

In the previous chapter a method is described which can be used to measure the kinetics of polyurethane polymerization for reactive extrusion purposes. Compared to common methods the method described offers in principle the advantage that measurements can be performed at high temperatures under mixing conditions, mimicking extrusion conditions. In the current chapter, this is investigated by comparing the results of other measurement methods for kinetics with the results of the kneader experiments.

Technique	Conversion range		Mixing	Temperature		
	Low (<98%)	High (>98%)	Yes / No	Low <60°C	Middle 60-140°C	High >140°C
Titration	+		No	+		
FT-ir	+		No	+	+	
ATR	+		Yes*		+	
SEC		+	No		+	+
NMR	+		No	+		
Fluorescence	+		No	+		
Rheometry	±	+	Yes		+	+

* Only premixing

Table 4.1 *Different kinetic measurement techniques.*

Several techniques have been used for the acquisition of data on kinetics (1, 2, 3, 4). Commonly used methods are titration, Fourier-transform infrared (FT-IR), adiabatic temperature rise (ATR) and size exclusion chromatography (SEC). Less common methods are fluorescence and NMR measurements. Unfortunately, the method applied often poses limits to the reaction conditions. In general, the reaction should not be too fast for all of these methods. Therefore, it is often necessary to keep the temperature and catalyst level low for the measurement of the kinetics. This limits the predictive window of the investigation, as reactive processing will usually occur

at high temperature and catalyst loading. In table 4.1, several techniques are compared. At first, the division of the conversion range in table 4.1 seems a little peculiar since the transition between 'low' and 'high' conversion is set at 98%. However, at this conversion the methods measuring the decrease of reactive groups become imprecise, while the methods that depend on the size of the molecules become more accurate above 98% conversion.

If we now look at the extrusion process for polyurethane polymerization, the monomers are fed to the extruder at a temperature of 60 - 80 °C. The temperature of the reaction mass increases rapidly in the first part of the extruder, mainly due to the fast exothermic reaction. Heat transfer through the wall and viscous dissipation are still of minor importance. For this part of the reaction, the reaction conditions more or less mimic adiabatic temperature rise measurements, although no mixing is present during adiabatic temperature rise experiments. However, the situation changes as soon as high molecular weight material appears. At that moment, the reaction velocity will have slowed down considerably (due to the second order nature of the reaction) and relatively little reaction heat will be generated. Furthermore, the temperature of the reaction mass will be well over 160 °C. In this regime, ATR-experiments will give a poor prediction of the reaction kinetics since the small heat of reaction will give a large error in the ATR-measurements. Methods based on molecular weight measurements, such as size exclusion chromatography or rheology, are more suitable in this situation.

Therefore, two different measurement methods seem necessary to establish the kinetics for the modeling of the polyurethane polymerization in an extruder. Of course, this is only the case if a different reaction temperature and different mixing condition result in a different behavior. In paragraph 4.2, this subject will be discussed in more detail.

Nevertheless, in the few studies on thermoplastic polyurethane extrusion that are known in literature (5 - 9) only a single method was used to measure the kinetics. Either adiabatic temperature rise measurements or size exclusion chromatography are used in these studies, inevitably leading to the described errors. The importance of these errors was investigated experimentally; the results are described in this chapter. The different methods will be compared with respect to the Arrhenius-behavior, the influence of the catalyst and the effect of mixing. Three different methods are surveyed: adiabatic temperature rise, size exclusion chromatography and kneader measurements. Two different thermoplastic polyurethane systems are investigated in order to further validate the number of

measurement methods that are required to determine the kinetics of polyurethane polymerization for reactive extrusion purposes.

4.2 Reaction Kinetics

For polyurethane polymerization, a few key phenomena may lead to a change in the observed activation energy and reaction rate with temperature and mixing:

- Different rate limiting steps may dominate at different temperatures, giving a change in activation energy and reaction rate. As explained in chapter 2.3.8, the multi-step reaction mechanism for the urethane formation is often condensed in a second order rate equation. This simplification may lead to erroneous extrapolation of the kinetics.
- Miscibility of the monomers. Due to the incompatibility of the monomers, an interfacial reaction will initially take place. If and how this affects the reaction will be described in paragraph 4.2.1.
- Diffusion limitation at high conversion. The reaction may slow down due to the appearance of large molecules. To what extent this affects the reaction will be described in paragraph 4.2.2.
- Phase separation. Phase separation of hard and soft segments (as described in paragraph 2.2) may give differences in local concentration of reactive groups. Moreover, the rigid hard segments may slow down the reaction rate by restricting the mobility of the molecules.
- Depolymerization. When the reverse reaction occurs (paragraph 2.3.4), as is the case at elevated temperatures, the observed reaction velocity will be slower. If this is not accounted for, an extrapolation of the result on kinetics will results in erroneous predictions.

4.2.1 Miscibility of the monomers

Due to incompatibility of isocyanate and alcohol molecules, the reaction will take place on and near the interface, and interfacial effects will influence the reaction. These interfacial aspects of polyurethane polymerization have been investigated in several publications (10 - 12). The starting point of these investigations was to evaluate the effect of impingement mixing, since many polyurethane products are made through a reactive injection molding processes where generally impingement mixing is an important process step. Kolodziej et al. (13) found that impingement mixing gives a dispersion with droplets that are still quite large (> 100 μm). An increase of the Reynolds number above 200 did not seem to decrease the droplet

size any further. This droplet diameter is far too high to result in a kinetically controlled reaction. A second process is necessary to overcome these limitations. This second (fast) mixing process seems to be related to surface instabilities. Machuga et al. (14) confirmed the observation of other authors that the polyol disappears more rapidly into the isocyanate than could be explained by pure diffusion. They found that the dimers that are formed on the boundary layer of the isocyanate and the polyol play an important role in this process. Probably, the urethane groups of these dimers undergo H-bond interactions with the isocyanate molecules across the border, resulting in strong surface destabilizing forces. It was found that the initial growth of the interfacial zone was independent of the monomers used. However, the further growth of this zone appeared to depend on the viscosities of the species that were present. Rigid oligomer molecules, a fast reaction, or the use of a crosslinking system limited the growth of the interfacial zone, which results in a diffusion controlled reaction. The effect of catalyst on the interfacial process is not clear. Wickert et al. (12) observed a much finer dispersion with catalyst than without, while Machuga et al. (14) detected no difference between catalyzed and uncatalyzed experiments.

4.2.2 Concept of functional group reactivity independent of molecule size

Another phenomenon that can have an effect on the polyurethane reaction is the concept of functional group reactivity independent of molecule size. For condensation polymerization reactions, it is normally assumed that the reaction rate constant and the reaction mechanism are constant for the entire reaction (15). The size of the molecules attached to a reactive group has no influence on the reaction rate. In other words, possible diffusion limitations will have no effect. To explain this it is assumed that a reactive group can be in two states: colliding with a different reactive group, or diffusing to a next reactive group. If a long molecule is attached to the reactive group, the diffusion time is longer, but the collision time is also longer. A reactive group will switch many times between these states before it actually reacts; therefore, the length of a molecule will not have a net effect on the reaction rate. This hypothesis is applied successfully in many cases. However, the theory does have a limitation; it does not hold for very long molecules or for very fast reactions. The theory has been verified with rather slow reacting systems ($t_{reaction}$ > 100 minutes). The polyurethane reaction is much faster, especially at higher temperatures. Whether this will result in a reaction that is diffusion limited can be verified experimentally.

4.3 Experimental

4.3.1 Chemicals used

Two different polyurethane systems were used in this investigation. The difference between both systems is the type of chain extender and the type of isocyanate used. The two systems were selected on the basis of the difference in compatibility of the chain extender and the isocyanate. This difference is expected to give a different behavior upon mixing. Where system 1 is a common TPU system, system 2 is easier to handle due to the liquid state of the isocyanate at room temperature. Both systems have the same amount of hard segments (24.0 %) and use the same catalyst (bismuth octoate). For all experiments, the pre-treatment of the monomers was as described in paragraph 3.2.2.

System 1:

- A polyester polyol of mono-ethylene glycol, di-ethylene glycol and adipic acid (MW = 2200 g/mol, f = 2)
- 1,4 butanediol (Mw = 90.1 g/mol, f = 2).
- 4,4 diphenylmethane diisocyanate (4,4-MDI). (Mw = 250.3 g/mol, f = 2).

System 2 (the same system as in chapter 3):

- A polyester polyol of mono-ethylene glycol, di-ethylene glycol and adipic acid (MW = 2200 g/mol, f = 2).
- Methyl-propane-diol (Mw = 90.1 g/mol, f = 2).
- A eutectic mixture (50/50) of 2,4 diphenylmethane diisocyanate (2,4-MDI) and 4,4 diphenylmethane diisocyanate (4,4-MDI). (Mw = 250 g/mol, f = 2).

Although the difference is not very large in the chemicals used in both systems, the differences that do exist may well result in a different reaction pattern. The following properties are affected:

- The polyol and diol are more compatible for system 2 than for system 1; therefore, the chain extender will dissolve at a lower temperature in system 2.
- The hard segments in system 1 will crystallize more readily. Both the differences in chain extender and in isocyanate contribute to that. In system 2 a methyl group on the chain extender will hinder the formation of a layered structure of hard segments. In addition, the non-linear 2,4-MDI that is present in system 2 will also be an obstacle for the crystallization of the hard segments.
- The compatibility of hard and soft segments in system 2 is also different to that of system 1. The use of methyl-propane diol as a chain extender in system 2 may influence the solubility of the hard and soft segments in a positive way.
- The polymer molecules formed are generally assumed to adapt a different conformation, depending on the system. While system 1 produces a completely linear molecule, the polymer molecules in system 2 will adopt a more staggered/coiled structure, due to presence of non-linear 2,4 MDI.
- The reactivity of the end groups of both systems may differ. We expect that the isocyanate group of 2,4-MDI that is placed in the ortho position will have a comparable reactivity to that of an isocyanate group in the para position. However, the approachability of the isocyanate group in the ortho position will be less due to steric hindrance. Therefore, the reactivity of the ortho-positioned isocyanate group may be lower than of the para-positioned isocyanate group. This difference in reactivity may lead to a lower overall reaction velocity.

4.3.2 Adiabatic Temperature Rise experiments

Adiabatic temperature rise (ATR) is a common method to measure the kinetics for polyurethane polymerization. With this method, the polyurethane kinetics at relatively low conversions and relatively low temperatures can be investigated. Many authors have described the experimental procedure for ATR measurements (1). The adiabatic reactor consisted of a paper cup (diameter = 5cm) surrounded by a layer of urethane foam for insulation. The reactor could be closed with a lid. The lid was equipped with a thin Copper Constantine thermocouple that stuck in the middle of the reaction mass when the lid was closed. The reaction mass was stirred with a turbine stirrer with a diameter of 4 cm. 200 grams (± 1 %) of material was used per experiment. To start an experiment, the necessary amounts of polyol and diol were

weighed in the reactor and mixed for 60 seconds with a turbine stirrer at 600 RPM. Care was taken to keep the temperature of the mixture above 60 °C, since demixing will take place at lower temperatures for both systems. The proper amount of catalyst was added with a syringe, and the polyol mixture was stirred for another 30 seconds. Finally, the proper amount of isocyanate was added with a syringe, and the reaction mass was stirred at 1500 RPM for 15 seconds. The cover was put on top of the reactor and the measurement was started.

Analysis of ATR results

In order to derive kinetic data from the ATR experiments, a simplified heat balance (equation 4.1) and rate equation (equation 2.12) were solved simultaneously (3, 11). For the heat balance, quasi-adiabatic conditions were assumed, since the reactor was not completely adiabatic for the time period under investigation. Depending on the reaction time, up to 4 % of the total reaction heat generated during the reaction was lost to the surroundings. The heat transfer coefficient h^* was obtained by fitting the cooling curves of several experiments, using equation 4.1. We took the density and the specific heat to be constant over the whole measurement range. Although both the specific heat and the density are somewhat dependent on the temperature, the temperature effects of both constants counteract, so that the net effect is negligible (< 5%). A non-linear regression method (error controlled Runge-Kutta) was used to solve the differential equations. With a least square routine, the difference between the model and the measurement was minimized. The calculations were performed with the software program Scientist.

$$V \cdot \rho \cdot C_p \cdot \frac{dT}{dt} = V \cdot \rho \cdot R_{NCO} \cdot \Delta H_R - h \cdot A \cdot (T - T_{room}) \quad \text{or}$$
$$C_p \cdot \frac{dT}{dt} = R_{NCO} \cdot \Delta H_R - h^* (T - T_{room}) \quad \text{with} \quad h^* = \frac{h \cdot A}{V \cdot \rho} \qquad (4.1)$$

$$R_{NCO} = \frac{d[NCO]}{dt} = R_{NCO,\,Uncat} + R_{NCO,\,Cat} = -k_f \cdot [NCO]^n$$
$$\text{with } k_f = A_{0,Uncat} \cdot e^{\frac{-E_{A,Uncat}}{R \cdot T}} + A_0 \cdot [Cat]^m \cdot e^{\frac{-E_A}{R \cdot T}} \qquad (2.12)$$

The fit procedure was as follows. Data obtained from the uncatalyzed runs on $E_{A,Uncat}$ and $A_{0,Uncat}$ were used as input parameters for the fit of the catalyzed runs. All the catalyst dependent runs were fitted simultaneously, giving the values for E_A, m and A_0. ΔH_R was taken from the experiment that gave the largest temperature rise.

Representation of the ATR results

Often the results of ATR measurements are plotted straightforwardly as the temperature versus the time. These plots give a clear view on $\Delta T_{adiabatic}$ and a global indication of the reaction velocity. A different method of plotting the results is to translate the temperature versus time plot into an Arrhenius-plot. Although it is much harder to visualize $\Delta T_{adiabatic}$ in such a graph, these plots give more information on the course of the reaction. The activation energy and the actual reaction velocity constants are better illustrated. Furthermore, the effect of the catalyst on the reaction velocity is clearly perceptible in these graphs. For an Arrhenius plot, the reaction rate constant must be known as a function of temperature. The reaction rate constant for an n-th order reaction can be calculated from an ATR experiment according to Richter and Macosko (16):

$$k_f = \frac{\rho \cdot C_p}{-\Delta H_R \cdot [NCO]_0^n} \cdot \left(\frac{\Delta T_{ad}}{\Delta T_{ad} + T_{t=0} - T} \right)^n \cdot \frac{dT}{dt} \qquad (4.2)$$

To account for the non-adiabatic conditions in our ATR reactor, the temperature versus time curve that is obtained in an ATR experiment is modified. This modified curve then serves as the basis for the calculation of the reaction rate constant (equation 4.2). To modify the curve, the amount of heat lost must be calculated for every time interval, starting at t = 0 (equation 4.3).

$$\Delta T_{loss} = \frac{h^*}{C_p} \cdot \Delta t \cdot \left(T - T_{room} \right) \qquad (4.3)$$

This temperature loss can be added to the measured temperature at that time interval. In this way, a modified ATR curve can be constructed.

4.3.3 High temperature measurements

A method to follow the conversion of a polyurethane polymerization at higher temperatures and conversions is for instance described by Ando et al. (17). In contrast to ATR experiments, this method is based on isothermal measurements. Small reaction flasks filled with premixed monomers are kept in a thermostatted oilbath. The polymer in the flasks is allowed to react for a certain time. Subsequently, the reaction is quenched and the samples are analyzed using size exclusion chromatography. The kinetic constants are then derived from a plot of the number average molecular weight versus time.

Two important conditions must be met in order to get meaningful results from this method. First, it is important that the reaction flasks reach the oilbath temperature much faster than the characteristic reaction time. For our experiments, an analysis based on the Fourier number revealed that this condition is met if the reaction time is larger than 15 minutes. This analysis does not take into account the reaction heat generated in the flasks. However, the reaction heat released only helps to reach the oilbath temperature sooner. Moreover, during the relevant part of the measurement, hardly any heat is generated.

A second condition that must be met to obtain relevant results is related to the analytical method. The molecular weight that is measured must represent the real molecular weight of the sample. Since our SEC equipment is calibrated with polystyrene samples, this requirement is not obvious. To check for this requirement, the samples of one experiment have been analyzed on a second SEC system. This second system was equipped with a triple detection system, so that the real molecular weight could be determined. A comparison of the results of the two systems revealed that the polystyrene calibrated system underestimated the weight average molecular weights ten to twenty percent. The difference in number average molecular weight was about ten percent. These errors are acceptable, which means that the results obtained on the polystyrene calibrated column can be used for our investigations on polyurethane kinetics.

Experimental procedure

The premixing procedure for these experiments was similar to that of the ATR experiments. However, the premixing time was extended to 40 seconds to ensure optimal mixing. After premixing, part of the reaction mass was transferred to small 1.5-ml reaction vials using a syringe. Subsequently submerging of the flasks in liquid nitrogen quenched the reaction temporarily. The total premix, fill and quench cycle took about two minutes. In the next step the flasks were capped while they were still frozen, the capping was carried out in a nitrogen atmosphere to prevent intrusion of moisture. The flasks were then submerged in a heated oilbath to restart the reaction. After the desired reaction time, a flask was transferred quickly into a beaker filled with liquid nitrogen. The flasks were broken and the content was dissolved in a 5% solution of di-butyl-amine in tetrahydrofuran (THF). Subsequently, the THF was evaporated. The samples obtained in this way were analyzed through size exclusion chromatography (18). The SEC-procedure used is described in the previous chapter (section 3.2.3). The experiments for system 1 were performed at five different temperatures (150, 160, 170, 180, and 200 °C). The effect of catalyst concentration was investigated at 150 °C. Furthermore, three different catalyst

levels were investigated (0.005, 0.015, 0.05 mg / g). The experiments for system 2 were performed at seven different temperatures (150, 160, 170, 180, 190, 200 and 210 °C). Every experiment was done at least once. The effect of catalyst concentration was investigated at 180 °C. Three different catalyst levels were investigated (0.1, 0.17, 0.3 mg / g).

Analysis of the experiments

The result of a high temperature experiment consists of a plot of the number average molecular weight versus time, an example is shown in figure 4.4. The *number* average molecular weight is taken as a measure of the conversion in these plots, because this average represents the amount of molecules present. For a second-order step-polymerization reaction, the number average molecular weight increases linearly in time (19):

$$M_N = M_{rep} \cdot \left(1 + [NCO]_0 \cdot k_f(T,[cat]) \cdot t\right) \qquad (2.15)$$

Strictly speaking, equation 2.15 is only valid for step-growth homopolymerizations with an A-B type of monomer. For the terpolymerization that we investigated, large deviations of this equation may occur, especially if the reactivities of the chain extender and the polyol are different (20). However, for the conversion range we investigated (> 95 %) the differences are negligible and, therefore, equation 2.15 is still suitable.

To derive the reaction rate constant k from an experiment, the initial slope of the curve has to be determined. A least square routine is used to establish this slope for each experiment. As follows from equation 2.15, the initial slope relates to the reaction rate constant according to:

$$k_f(T,[cat]) = \frac{dM_N}{dt} \cdot \frac{1}{M_{rep} \cdot [NCO]_0} = slope \cdot \frac{1}{M_{rep} \cdot [NCO]_0} \qquad (4.4)$$

In this way, the reaction rate constants can be obtained at different temperatures. The initial slope is used to derive the reaction rate constant, since the number average molecular weight will not increase indefinitely over time.

For each temperature, the equilibrium molecular weight can also be established with high temperature experiments. This value can be used to calculate the equilibrium constant and the reverse reaction rate at that temperature (equation 2.17).

$$K = \frac{k_f}{k_r} = \frac{[U]_{eq}}{[NCO]_{eq}^2} = \frac{\overline{M}_N \cdot \left(\overline{M}_N - M_0\right)}{M_0^2 \cdot [NCO]_0} = A_{0,eq} \cdot e^{\frac{E_{A,eq}}{R \cdot T}} \qquad (2.17)$$

The experimental graphs (e.g. figure 4.4) show that there is some scatter in the value for the equilibrium molecular weight. Therefore, an average equilibrium molecular weight is taken for every temperature. In figure 4.4, the shaded areas indicate which part of the curve is considered to be in equilibrium.

4.3.4 Kneader experiments

The third method to measure the kinetics of polyurethane polymerizations with a measurement kneader has been described in chapter 3. Experiments were performed at four different temperatures (125, 150, 175, 200 °C). The effect of the catalyst concentration was investigated at 175 °C. Four different catalyst levels were used (0.25, 0.40, 0.75 and 1.30 mg / g). For system 1 and 2 the same experiments have been performed. All experiments were repeated three times. The results of these experiments will be discussed in the result section.

4.4 Results

The result section is split into different parts. The results of each measurement method are discussed separately, and for each method, the two different urethane systems are compared. Subsequently, the measurement methods are compared for every system, in order to see if they really result in different kinetic data.

4.4.1 Adiabatic temperature rise measurements

Typical graph

As discussed in the experimental section, the ATR results are shown in an Arrhenius plot. Figure 4.1 shows the results of a duplicate experiment for system 1 and 2. The same catalyst level is used for both systems. A second order reaction rate equation is adopted to construct figure 4.1. This assumption seems to be valid for both systems. If we compare both graphs, it is clear that system 1 reacts about one and a half times faster than system 2. As expected, the reaction rate does not rise to infinity; the reaction slows down considerably at a certain conversion. In figure 4.1, this is visible at the point where the tangent line deviates from the measurement points. Surprisingly, the conversion at that point is still quite low, for both systems between 65 and 70 %. A comparison of all experiments showed that regardless of the catalyst level, the decrease in reaction velocity starts between 65

and 70 % for both systems. The reaction does proceed after that point, but the reaction rate constant continues to decrease at higher conversions. The reason for the decrease of the reaction rate constant is not immediately clear. The decrease is too large to attribute it to a change in the reaction order.

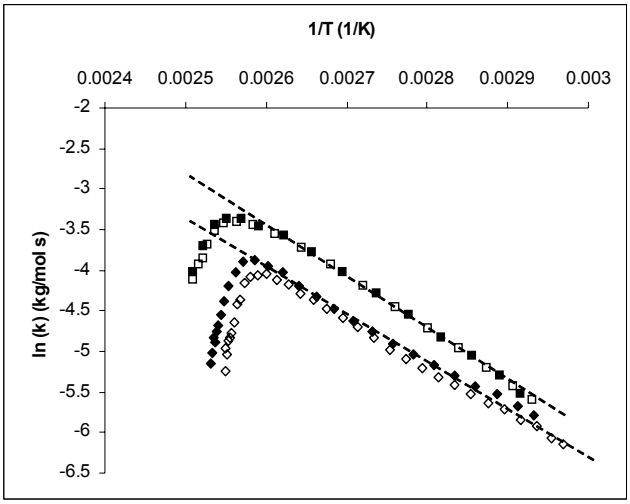

Figure 4.1 *ATR experiments. [Cat] = 0.075 mg/g, ■ / □ system 1, ♦ / ◇ system 2.*

As explained in the theoretical section, the reaction may slow down due to diffusion effects. However, the average degree of substitution at 70 % conversion is about equal to three, for linear homopolymers this would be too low to give rise to a large diffusion resistance. Nevertheless, for polyurethanes, phase separation of hard and soft segments may be the cause of the drop in reaction velocity. Due to the clustering of the hard segments, the mobility of the molecules decreases considerably, this can decrease the observed reaction velocity. Blake et al. (21) showed that for fast ATR experiments, the onset of the phase separation is dependent on the initial temperature, catalyst level and the hard segment percentage. They found that phase separation occurred between 66 % and 90 % conversion, which is in agreement with our observations. However, contrary to Blake et al. (21), we do not see an effect of the catalyst concentration on the position of the onset point. This can be explained by the fact that our experiments are much slower. In that case, the phase separation kinetics will be much faster than the reaction kinetics, regardless of the catalyst level. In other words, in our case the phase separation rate does not limit the rate of reaction. Surprisingly, also the chemical composition seems to have no influence on the onset point, since both

systems show the same effect at the same conversion. Possibly, the structure of the hard segments does not differ largely for our systems, in spite of the difference in chain extender and isocyanate.

In many ATR investigations, the effect of phase separation on the reaction velocity has not been observed. However, these investigations often use a higher hard segment percentage, which increases the temperature at which the phase separation takes place (21). Since at higher conversions the reaction becomes difficult to follow (due to the decrease in heat generation at high conversions) the effect of phase separation may be less visible, which would explain the lack of data. In ATR studies using cross-linking polyurethane systems, a decrease in reaction velocity has been observed at higher conversions (21, 22). Contrary to phase separating systems, the mobility of the molecules for these systems is limited due to crosslinking at higher conversions, instead of clustering of the hard segments. Cross-linking already takes place at a conversion of 70%, this makes the effect much easier to detect.

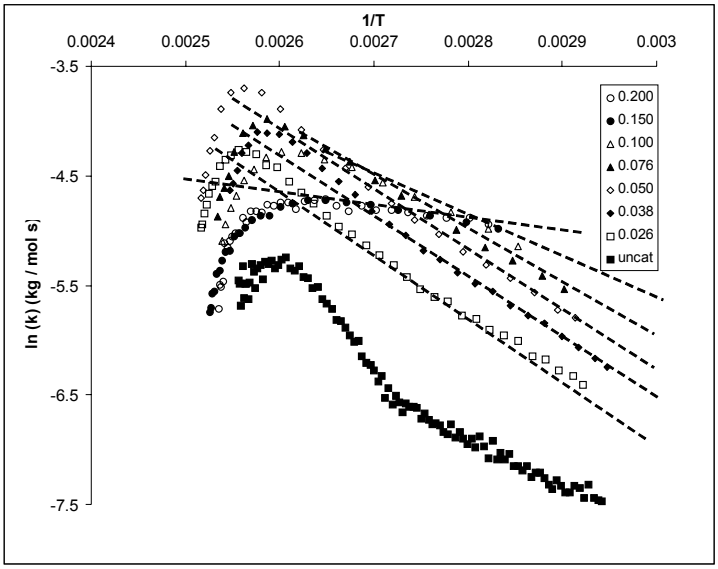

Figure 4.2 *ATR experiments. Catalyst dependence of system 2.*

Comparison of different catalyst levels

In figure 4.2 and 4.3, the experiments at different catalyst levels are shown. The zero catalyst experiments are much slower than the runs with the lowest catalyst level (3 - 6 times for system 1, 2 - 4 times for system 2).

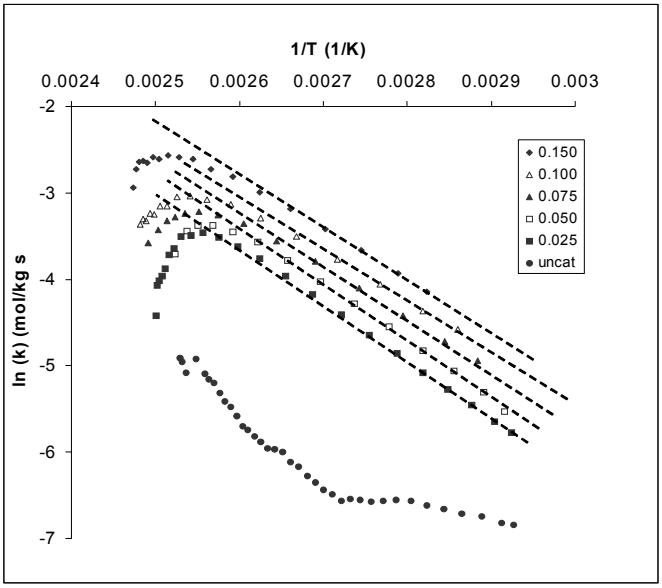

Figure 4.3 *ATR experiments. Catalyst dependence of system 1.*

However, the reaction path of the uncatalyzed runs can hardly be compared with those of the catalyzed runs. As mentioned in the theory, the isocyanate droplets may disperse much finer in the presence of catalyst. In case the catalyst is absent, the then occurring larger droplets will result in a more pronounced diffusion limitation for the initial part of the reaction. This explains the low initial activation energy of the uncatalyzed runs (20 kJ/mol for system 1, 35 kJ/mol for system 2). Nevertheless, at a certain conversion, the oligomers formed are likely to compatibilize the reaction mass, resulting in a less diffusion-limited reaction and in a higher activation energy (± 100 kJ/mol mol for system 1, 75 kJ/mol for system 2). This would explain the sudden increase in activation energy in figures 4.2 and 4.3. An autocatalytic process might also be responsible for the sudden increase of the reaction velocity. However, repeated experiments showed that the uncatalyzed runs were very sensitive to mixing, which supports the mixing hypothesis. A model fit of the uncatalyzed runs will be imprecise due to this mixing sensitivity, especially since the activation energy increases suddenly during the reaction. Still a fit of the uncatalyzed runs was used in this kinetic study, since the uncatalyzed reaction contributes to some extent to the overall reaction velocity.

Now, if we look at the catalyzed runs, the experiments for system 2 show a remarkable behavior. Normally, one would expect the reaction velocity to increase with increasing catalyst level, while the activation energy remains the same.

However, if we look at figure 4.2, it seems that the activation energy decreases with increasing catalyst level, whereas the initial reaction velocity increases with catalyst level, as expected. For system 1, this behavior does not occur (figure 4.3). Therefore, the cause for this phenomenon must be found in the structure of the monomers of system 2. The 2,4-MDI in system 2 results in staggered oligomer and polymer molecules (as explained in the theoretical section). Staggered or rigid molecules hinder the formation of a broad interfacial zone of isocyanate and polyol. Only if this layer is present the mixing will be so fast that the reaction is kinetically limited. According to Machuga et al. (16), the initial growth of this zone will be the same for all catalyst levels. In that case, the reaction velocity depends on the catalyst concentration in the interfacial zone, resulting in an initial reaction velocity that is catalyst dependent. However, at higher catalyst levels the growth rate of the intermaterial zone decreases or even stops, due to the faster formation of large, viscous molecules. Therefore, the combination of staggered molecules and high catalyst level may result in incomplete micromixing of the reactants. The resulting diffusion limitation is observable in an Arrhenius plot as a decrease in activation energy with increasing catalyst level. In figure 4.2, the activation energy continues to decrease with higher catalyst concentrations until the maximum in reaction velocity is reached at high catalyst levels (0.15 and 0.20 mg/g). As a result, two different sets of kinetic parameters needed to be determined for system 2. The runs with the lowest four catalyst levels (0.025 – 0.075 mg / g) were used to establish the kinetic constants for the experiments at a low catalyst level (the fitting procedure can be found in the experimental section). However, due to the inconsistency in activation energy of system 2, a second set of parameters was necessary to model the reaction at high catalyst levels. Therefore, the highest two catalyst level runs were used to establish a catalyst-independent rate equation, since these experiments were found to be equally fast, regardless of the catalyst concentration. The results are shown in table 4.1.

System 1	ATR		High Temperature Experiments	Kneader Experiments
A0, Uncat (kg/mol s)	169.1			
EA, Uncat (kJ/mol)	35.3			
A0 (kg/mol·s) ·(g/mg)m	1.25e6		$2.69 \cdot 10^{6}$	$5.13 \cdot 10^{5}$
m (-)	0.61		0.5	0.57
EA (kJ/mol)	50.5		53.6	52.0
System 2	ATR low [cat]	ATR high [cat]	High Temperature Experiments	Kneader Experiments
A0, Uncat (kg/mol·s)	5.37e3			
EA, Uncat (kJ/mol)	45.8			
A0 (kg/mol·s) ·(g/mg)m	1.09e5	0.208	$1.49 \cdot 10^{7}$	$2.18 \cdot 10^{6}$
m (-)	0.92	0	0	0
EA (kJ/mol)	42.5	9.9	71.9	61.3

Table 4.1 *The kinetic parameters for system 1 and 2.*

In contrast to system 2, the Arrhenius plot for system 1 (figure 4.3) shows a regular behavior. At a higher catalyst level, the activation energy remains constant whilst the reaction rate constant increases, indicating that no diffusion limitations occur unlike system 2. Using figure 4.3, a fit has been made according to the fitting procedure as described in the experimental section. The resulting model parameters are also shown in table 4.1.

4.4.2 High conversion experiments

A typical graph for a high conversion experiment is shown in figure 4.4. Two experiments and their duplicates are shown. System 2 was used for these experiments. The solid lines represent the model predictions; the model predictions are based on a fit of all high temperature experiments performed in this research. The resulting parameters describing the kinetics are shown in table 4.1. As expected, the molecular weight increases in time. Initially, the increase is linear. This part of the curve is used to determine the initial slope. At longer reaction times, the molecular weight levels off due to depolymerization. At both temperatures, the reproducibility of the experiments is reasonable.

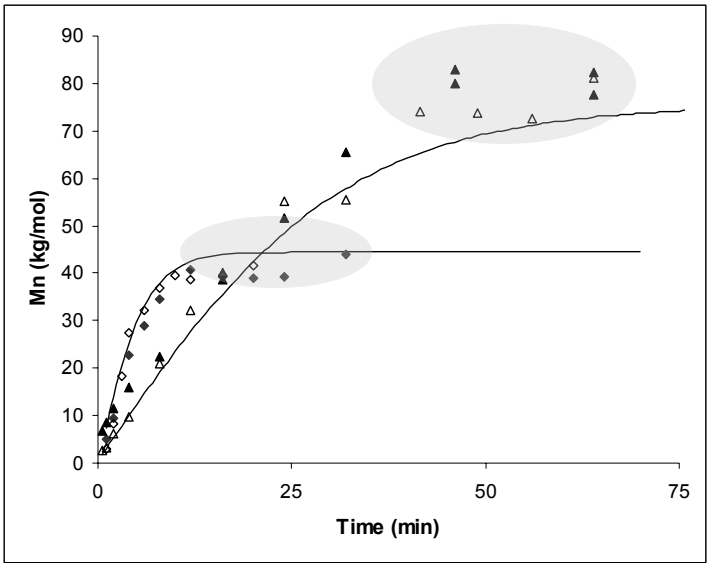

Figure 4.4 *M_n versus time for the high temperature experiments for system 2, experimental results and model prediction. ◢150 °C, Δ 150 °C duplicate, ◆ 200 °C, ◇ 200 °C duplicate. The points in the grey areas are used to determine the equilibrium molecular weight.*

The procedure to derive the kinetic data is described in the experimental section. This procedure is used to obtain the forward and reverse reaction rate at every temperature under investigation.

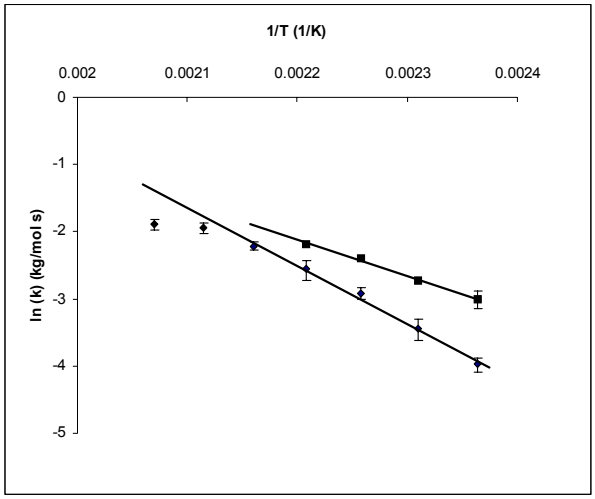

Figure 4.5 *The forward reaction rate constant as a function of temperature for high temperature experiments.* ■ *system 1,* ♦*System 2.*

In figure 4.5 an Arrhenius plot of the forward reaction rate is shown for all experiments performed with system 1 and 2. At lower temperatures both systems exhibit a linear relationship between ln(k) and 1/T, which confirms the second order rate assumption. However, for system 2 a deviation from linearity turns up at higher temperatures (200 ˚C, 210 ˚C). This is due to the fact that the slopes of these curves are determined largely during the first 15 minutes of the reaction, when the flasks are still warming up (as explained in the theoretical section). Therefore, the effective flasks temperature will be lower than the oilbath temperature, which explains the downward curvature in figure 4.5. For this reason, the experiments at 200 and 210 ˚C are not used to determine the Arrhenius-parameters for system 2. However, the runs at 200 and 210 ˚C can still be used to determine the kinetics of the depolymerization reaction.

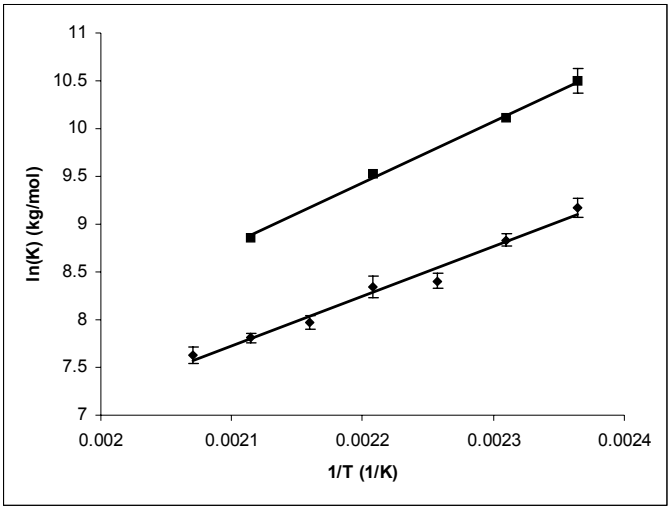

Figure 4.6 *The equilibrium constant as a function of temperature for high temperature experiments.* ■ *System 1,* ♦ *system 2.*

The equilibrium molecular weights are determined at reaction times larger than 15 minutes, which makes sure that the flasks have reached the oilbath temperature. In figure 4.6 the Arrhenius plot for the depolymerization reaction is shown for system 1 and 2.

	System 1	System 2
Aeq (kg/mol)	0.0110	0.0393
EA,eq (kJ/mol)	52.7	43.4

Table 4.2 *The equilibrium parameters for system 1 and 2.*

The equilibrium constant for each temperature is calculated by substituting the equilibrium molecular weight in equation 2.17. The plot shows that even at 150 ˚C the effect of depolymerization is noticeable. The resulting parameters for the depolymerization reaction are presented in table 4.2. Besides the effect of depolymerization, the effect of the catalyst concentration was also investigated through high conversion experiments. For system 2, the catalyst level did not have an effect on the reaction rate constant, at least not for the relatively high catalyst levels that were chosen. For system 1, the reaction rate was about proportional to the square root of the catalyst concentration (table 4.1).

4.4.3 Kneader Experiments

The results of the kneader experiments for system 2 were discussed in a previous chapter. However, in this chapter only one catalyst level was used. Therefore, additional experiments were performed to establish the catalyst dependence for both systems. The resulting plots of reaction rate versus catalyst concentration are shown in figure 4.7.

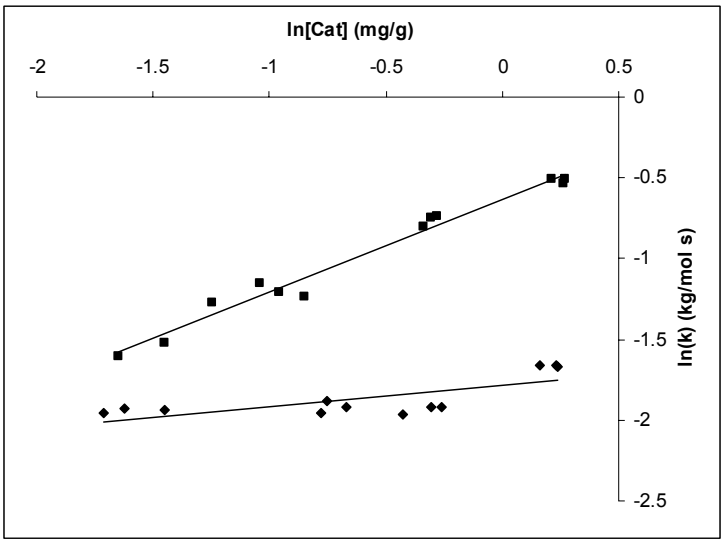

Figure 4.7 *The dependence of the Arrhenius pre-exponential constant on the catalyst level.* ■ *System 1,* ♦ *System 2.*

For system 2, the experiments at the highest catalyst level are slightly faster than the other three experiments, indicating that there is a slight influence of catalyst concentration on the reaction velocity. This influence is very small, and since the other three catalyst levels do not show any effect of the catalyst, the reaction velocity is considered independent of the catalyst concentration. For system 1 the catalyst dependence is obvious, the dependency factor m in equation 2.12 is equal to 0.57. More discussion on the effect of catalyst will follow in the next sections. Furthermore, figure 4.7 shows that system 1 reacts faster than system 2 at all catalyst levels. As explained in the theoretical section, the 2,4- MDI that is used in system 2 may cause it to react slower. The effect of the temperature on the reaction velocity for system 1 is shown in figure 4.8. Analogous to system 2, the model predictions and the experimental curves are shown, and the kinetic constants are obtained in a similar way as for system 2 (18).

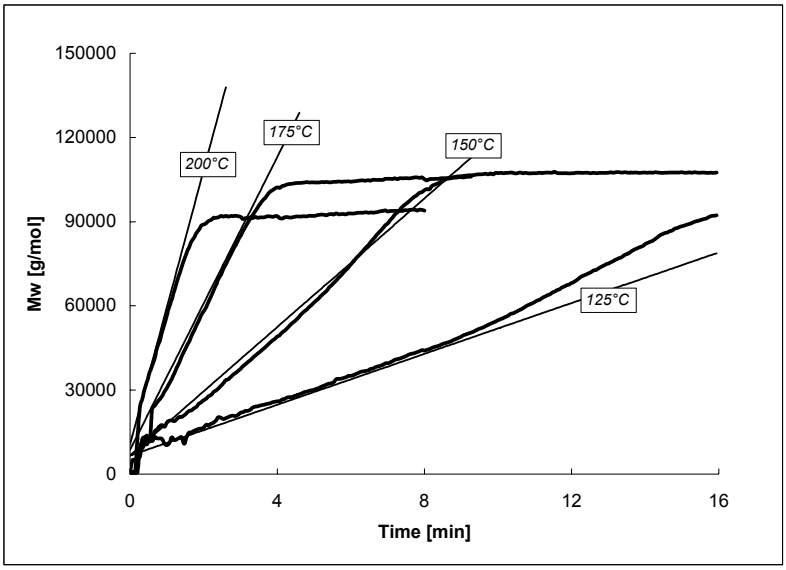

Figure 4.8 *The Mw versus time for the kneader experiments for system 1. 80RPM. Model predictions and experimental results.*

4.4.4 Comparison of the different measurement methods, System 1

Table 4.1 shows a comparison of all the kinetic parameters obtained for system 1. Both the catalyst dependence and the activation energy seem to agree fairly well for all experimental methods. This observation indicates that for all measurement methods used, the reaction develops identically for system 1. Neither the activation energy nor the catalyst dependence changes appreciably with the temperature-range or the conversion-range of the measurement method. The simplified second order assumption seems to hold for all measurement conditions. If we look at the catalyzed urethane reaction, the reaction develops through several equilibrium steps, all related to the catalytic center. Naturally, these equilibriums will shift with temperature, which may change the reaction order and catalyst dependence. Surprisingly, both the reaction order and the catalyst dependence remain constant for the temperature range under investigation. The order of catalyst dependence (≈ 0.5) falls within the limits reported by other authors (0.5 – 1). A possible explanation for the value of 0.5 for the order of catalyst dependence is given by Richter et al. (16). They related this value to a simple reaction mechanism. In the first step of this mechanism, the catalyst dissociates and, in a second step, the

cationic catalytic center forms a complex with an isocyanate group. If both steps are thermodynamically unfavorable, the reaction order equals 0.5.

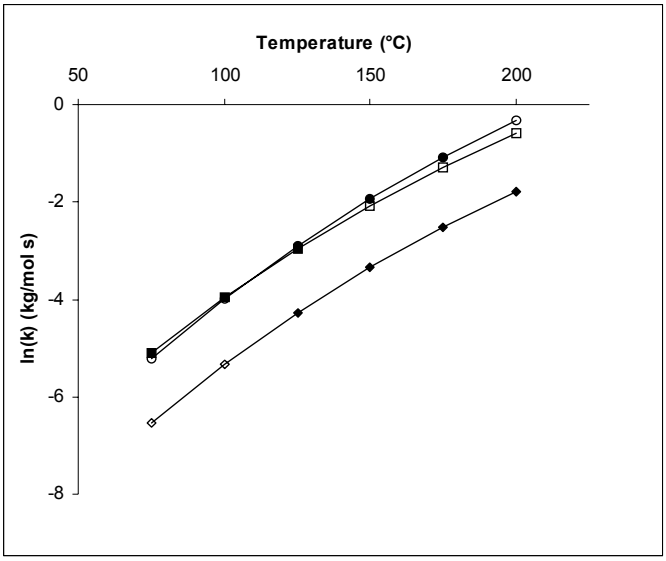

Figure 4.9 *The model reaction rate constant versus the temperature for the different measurement methods. System 1. The open symbols are extrapolations to areas where no measurements have been carried out.* ■ *ATR,* ♦ *kneader,* ● *high temperature.*

The effect of the different measurement methods on the reaction rate constant is shown in figure 4.9. Figure 4.9 shows that the ATR experiments are as fast as the high temperature experiments. Within the experimental error, for these two types of measurements, the method does not seem to have any influence on the observed reaction rate. A priori, one would expect the kneader experiments to be equally fast, or even faster than the high temperature experiments. However, the kneader experiments show reaction rate constants that are 3-4 times slower. No obvious explanation is available to account for this result. The mysterious drop in reaction velocity may be attributed to the materials used. The only difference between the kneader experiments and the other two experiments is the batch of polyol and chain extender used. The acidity and OH-value, which have an effect on the reaction rate, may change per batch of polyol. No corrections were made for these changes.
Due to the use of a different polyol batch, no valid comparison can be made between the kneader experiments and the other two types of experiments. However, the other two experiments do give important information on the polyurethane

reaction. The observation that the reaction velocity does not depend on the measurement method deployed implies that the theory of functional group reactivity independent of chain length is also valid for polyurethanes. Moreover, it strengthens the belief that for the ATR and high temperature experiments (initial) diffusion limitations do not occur, since the reaction velocity, the reaction order and the catalyst dependence is the same for both experiments. For extruder applications, the result means that the most convenient measurement method can be chosen to obtain the correct data for the kinetics, at least for this polyurethane system. The advantage of ATR experiments is the ease of measurement; on the other hand, the high temperature experiments give essential information on the depolymerization reaction.

4.4.5 Comparison of the different measurement methods, System 2

Similar to system 1, two batches of materials were used for the experiments of system 2. The ATR experiments for system 2 were performed with the same batch of polyol as the ATR experiments and high temperature experiments of system 1. The kneader and the high temperature experiments were performed with the other batch of polyol, which is also used for the kneader experiments of system 1. In table 4.1 the same batches have the same color. Again, possible inconsistency in batches complicates the comparison of the different experiments. Moreover, the specific diffusion limitations that were observed for the ATR experiments make comparison of this method with the other two methods even harder. These diffusion limitations are specific for the ATR method (and for the polyurethane system used), and result in a catalyst-independent reaction velocity at higher catalyst levels, and a lowering of the activation energy. For the high conversion experiments, the lack of catalyst dependence is also observed at higher catalyst levels, but the activation energy is much higher for these experiments. Therefore, the cause of the catalyst independency for these experiments must be different. An obvious explanation is not available, possibly the functional groups of the polymer molecules experience a diffusion limitation that is noticeable at higher catalyst levels. In that case, the catalyst level does not make any difference above a certain threshold concentration. This explanation is not completely satisfactory. First, this type of diffusion limitation does not occur for system 1. However, the difference in monomers for the two systems might give a difference in the polymer structure and therefore in diffusion behavior. The staggered 2,4-MDI groups in system 2 may result in a more coiled polymer molecule which subsequently can result in a more ‘entangled’ polymer melt in which diffusion limitations occurs more readily. Still, a

second question remains. The activation energies that are found for the high conversion experiments are rather high for a diffusion-limited reaction (60 – 70 kJ/mol). The flow activation energy for system 2, which can be considered as the activation energy of diffusion, is much lower: 43 kJ/mol (18). The reason for this difference is not clear.

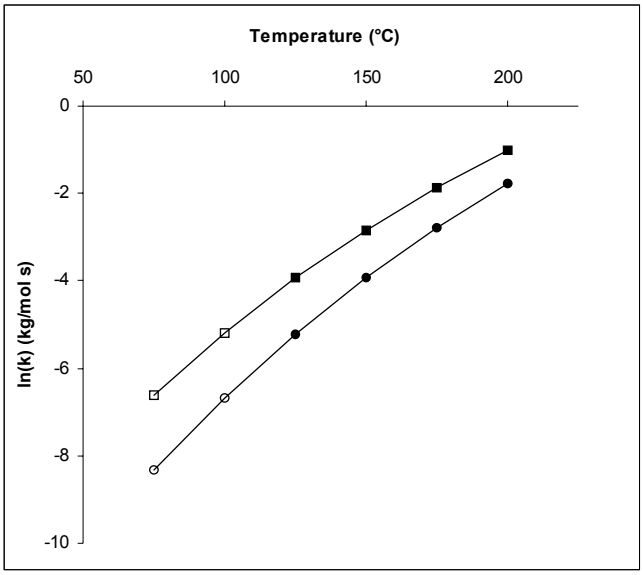

Figure 4.10 *The reaction rate constant versus the temperature for the different measurement methods. System 2. The open symbols are extrapolations to areas where no measurements have been carried out.* ■ *Kneader,* ● *high temperature.*

Now, if we look at the difference between the two high conversion methods, mixing seems to have an influence. Both experiments are performed with the same batch of polyol; therefore, a comparison can be made. The kneader experiments show a much higher reaction rate constant than the high temperature experiments (figure 4.10). This observation may support the assumption that the reaction for system 2 is subject to diffusion limitations. Mixing in that case alleviates the diffusion limitation, resulting in a faster reaction.

4.5 Conclusions

The reaction kinetics of polyurethane polymerization was studied in this chapter. In particular, the need for different measurement methods for reactive extrusion purposes was investigated. The study shows that ATR and high temperature measurements give the same kinetic constants for a commercial polyurethane system (system 1). Since both methods differ greatly in reaction time, reaction temperature, and analytical method, it can be concluded that for this system both measurement methods can be applied. Unfortunately, an extra validation of this conclusion with a third method (with the measurement kneader) could not be used, since a different batch of polyol had to be used for these last measurements. However, the activation energy, catalyst dependence and reaction order was similar for the kneader experiments, which strengthens the vision that any of the three measurement methods will yield the same kinetic equation for system 1. Therefore, it is probable that the reaction is kinetically controlled and that the reaction proceeds uniformly over a wide range of temperatures and conversions.

For a less common polyurethane system (system 2), a completely different result is obtained. The three different measurement methods each result in a different kinetic equation, indicating that for this system a uniform reaction mechanism cannot be adapted. For extrusion purposes, this means that a single kinetic measurement method does not suffice. At least two measurement methods seem to be required; a low temperature, low conversion method as adiabatic temperature rise experiments and a high temperature high conversion method.

The cause of these inconsistencies may result from the structure of the monomers used in system 2. As explained in the result section, the presence of 2,4-MDI in system 2 may hinder the expansion of surface instabilities (which are indispensable for good micromixing) and therefore prevent a kinetically controlled reaction (14). However, since this hypothesis is only derived from the kinetic parameters for this system, a further validation would be necessary; for example by following the reaction under a microscope.

4.6 List of Symbols

A_0	Reaction pre-exponential constant	mol/kg s
A	Surface area of ATR reactor	m^2
[Cat]	Catalyst concentration	mg/g
C_p	Heat capacity	J/kg·K
E_A	Reaction activation energy	J/mol
ΔH_R	Heat of reaction	J/mol
h	Heat transfer coefficient	$J/m^2 \cdot s \cdot K$
h^*	Overall heat transfer coefficient	J/kg·s·K
k_f	Forward reaction rate constant	kg/mol·s
k_r	Reverse reaction rate constant	1/s
m	Catalyst order	-
M_0	Average weight of repeating unit	g/mol
M_N	Number average molecular weight	g/mol
M_W	Weight average molecular weight	g/mol
n	Reaction order	-
[NCO]	Concentration isocyanate groups	mol/kg
$[NCO]_0$	Initial concentration isocyanate groups	mol/kg
ρ	Density	kg/m^3
R	Gas constant	J/mol K
R_{NCO}	Rate of isocyanate conversion	mol/kg·s
T	Temperature	K
ΔT_{ad}	Adiabatic temperature rise	K
t	Time	s
[U]	Concentration urethane bonds	mol/kg
V	Volume ATR reactor	m^3

Subscripts

Cat	Catalyzed
Uncat	Uncatalyzed
Eq	Equilibrium

4.7 List of References

1. C. W. Macosko, RIM - Fundamentals of Reaction Injection Molding, Hanser, Munich, (1989).
2. P. Cassagnau, F. Mélis, and A. Michel, J. Appl. Polym. Sci., **65**, 2395 (1997).
3. X.D. Sun, and C.S.P. Sung, Macromolecules, **29**, 3198, (1996).
4. X. Sun, J. Toth, and L.J. Lee, Polym. Eng. Sci., **37**, 143 (1997).
5. P. Cassagnau, T. Nietsch and A. Michel, Intern. Polym. Process., **14**, 144 (1999).
6. M.E. Hyun, and S.C. Kim, Polym. Eng. Sci., **28**, 743 (1988).
7. A. Bouilloux, C.W. Macosko, and T. Kotnour, Ind. Eng. Chem. Res., **30**, 2431 (1991).
8. S. Hoppe, S. Grigis, and F. Pla, Chisa 2002 A53
9. G. Lu, D.M. Kalyon, I. Yilgör, and E. Yilgör, Polym. Eng. Sci., 388 (2003)
10. S.D. Fields, E.L. Thomas, and J.M. Ottino, Polymer, **27**, 1423 (1986).
11. S.D. Fields, and J.M. Ottino, AIChE J., **33**, 959 (1987).
12. P.D. Wickert, W.E. Ranz, and C.W. Macosko, Polymer, **28**, 1105 (1987).
13. O. Kolodziej, C.W. Macosko, and W.E. Ranz, Polym. Eng. Sci., **22**, 388 (1982).
14. S.C. Machuga, H.L. Midje, J.S. Peanasky, C.W. Macosko, and W.E. Ranz, AIChE J., **34**, 1057 (1988).
15. P.J. Flory, Principles of Polymer Chemistry, Cornell University Press, Ithaca, N.Y., (1953).
16. E.B. Richter, and C.W. Macosko, Polym. Eng. Sci., **18**, 1012 (1978).
17. T. Ando, Polym. J., **11**, 1207 (1993).
18. V.W.A. Verhoeven, M. van Vondel, K.J. Ganzeveld, and L.P.B.M. Janssen, Polym. Eng. Sci., **44**, 1648 (2004)
19. G. Odian, Principles of Polymerization, John Wiley & Sons Inc., New York (1991).
20. F. Lopez-Serrano, J.M. Castro, C.W. Macosko, and M. Tirrell, Polymer, **21**, 263 (1980).
21. J.W. Blake, W.P Yang, R.D. Anderson, and C.W. Macosko, Polym. Eng. Sci., **27**, 1237 (1987).
22. Y.T. Chen, and C.W. Macosko, J. Appl. Polym. Sci., **62**, 567 (1996).